# Heat treatment during composite extruded spring steel wire reinforced EN AW-6082

**Andreas Reeb, Matthias Merzkirch, Volker Schulze, Kay A. Weidenmann**

**Angaben zur Veröffentlichung / Publication details:**

Reeb, Andreas, Matthias Merzkirch, Volker Schulze, and Kay A. Weidenmann. 2016. "Heat treatment during composite extruded spring steel wire reinforced EN AW-6082." *Journal of Materials Processing Technology* 229: 1–8.
https://doi.org/10.1016/j.jmatprotec.2015.08.022.

# Heat treatment during composite extruded spring steel wire reinforced EN AW-6082

Andreas Reeb*, Matthias Merzkirch, Volker Schulze, Kay André Weidenmann

*Karlsruhe Institute of Technology (KIT), Institut für Angewandte Materialien – Werkstoffkunde (IAM–WK), Engelbert-Arnold-Strasse 4, 76128 Karlsruhe, Germany*

## 1. Introduction

In the field of transportation, lightweight structures with high specific strength and stiffness are needed in order to save energy and natural resources. Therefore metallic light alloys reinforced with stiff and strong wires are adequate materials to meet this requirement. The composite extrusion process, which principle is described in Kleiner et al. (2007), allows for a direct embedding of stiff and strong wires into a metallic matrix to produce a variety of unidirectional reinforced profiles with different variants of reinforcement as demonstrated by Pietzka et al. (2008) and multiple geometries shown in Pietzka and Tekkaya (2009). Pietzka (2013) and Dahnke et al. (2014) showed that up to now the extrusion of profiles with a reinforcing volume of 13.5 vol.-% is feasible. Maximum reinforcing volume possible is restricted by pressing force on hand and geometric restrictions and was determined to a theoretical maximum of 31 vol.-% by Pietzka (2013). For structural applications a further enhancement of the mechanical properties is desirable. By integrating heat treatment steps like solutionizing and quenching into the extrusion process, the full potential of hardenable aluminium alloys can be exploited. The regarded aluminium alloy EN AW-6082 (AlMgSi1) is a medium-high strength wrought alloy which allows for precipitation hardening by forming metastable $Mg_2Si$ ($\beta'$)-precipitations which is described in detail by Edwards et al. (1998) and Murayama and Hono (1999). Lim and Shercliff (1993) investigated the quench sensitivity of this alloy and stated that quenching with water after solutionizing is necessary in order to reach optimized peak aged condition. Mrówka-Nowotnik and Sieniawski (2005) studied the influence of heat treatment on the mechanical properties and could approve the quench sensitivity of the EN AW-6082 alloy. Therefore, with a well-adapted heat treatment to the matrix material, a significant gain of specific strength is expected. In order to reduce processing time, save energy and reduce possible negative effects on the bonding zone between wire and matrix, like shown by Pattnaik and Lawley (1974) the heat treatment process was integrated into the composite extrusion process with a newly developed quenching setup for water quenching of the extrusion profiles. The current contribution deals with the investigation of the influence of different quenching methods and subsequent heat treatment processes on the mechanical properties in tensile loading and interfacial shear strength of a unidirectional 11.1 vol.-% spring steel wire reinforced EN AW-6082 (AlMgSi1) matrix composite. A detailed investigation of the deformation and damage behaviour of spring steel reinforced

* Corresponding author. Fax: +49 721 6084 8044.
*E-mail address:* andreas.reeb@kit.edu (A. Reeb).

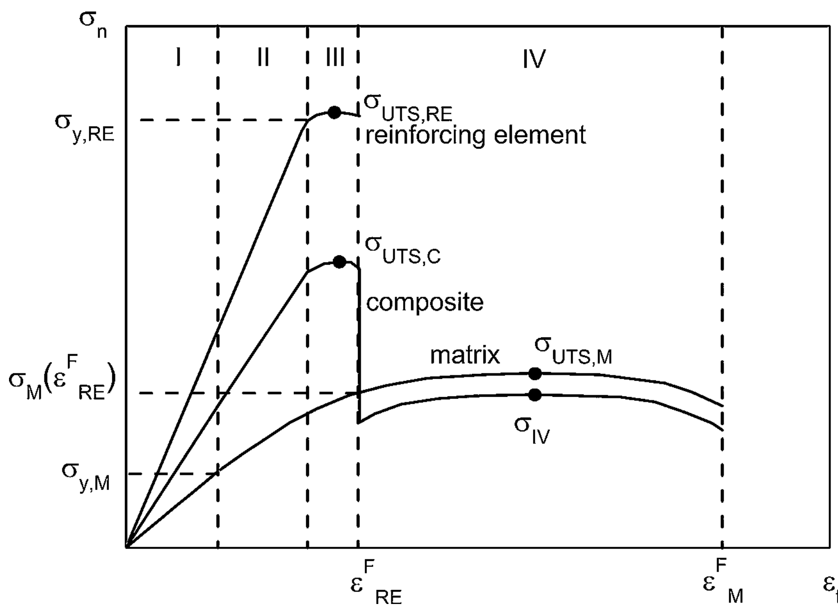


**Fig. 1.** Schematic stress-strain diagram for a composite consisting of a ductile matrix and a ductile reinforcement calculated from the mechanical behaviour of its components according to Weidenmann et al. (2006a).

EN AW-6082-T4(F) was done by Merzkirch et al. (2011, 2014); Merzkirch (2012) and is compared to the results of this work.

### *1.1. Principles of tensile behaviour of unidirectionally reinforced MMC*

Based on the investigations of Voigt (1887) the tensile behaviour of unidirectionally reinforced composites is discussed in detail by Kelly and Davies (1965) and Courtney (2000) using the stress-based rule of mixture. Altogether four regions of deformation and damage can be described which are shown in Fig. 1.

Within region I pure elastic behaviour is shown where the rule of mixture for the Young's modulus $E_I$ can be used. The beginning of region II is defined by the onset of plastification of the matrix material at its yield strength $\sigma_{y,M}$. The superposition of the elastic behaviour of the reinforcing element and the elastic-plastic behaviour of the matrix material within region II can be approximated by Eq. (1):

$$E_{II} = E_{RE} \times V_{RE} + \left(\frac{d\sigma_M}{d\epsilon_M}\right) \times V_M \quad (1)$$

The differential coefficient $\left(\frac{d\sigma_M}{d\epsilon_M}\right)$ describes the slope of the stress-strain curve after onset of plastification and marks the linear approach of the hardening of the unreinforced matrix material. Since the slope during hardening is low in comparison to the Young's modulus of the reinforcing element, Eq. (1) can be simplified by neglecting the second term. Region III is determined by the plastification of the reinforcing element and does not occur where brittle reinforcing elements are used, as shown by Kelly and Davies (1965) and Courtney (2000). The ultimate tensile strength of the composite can be calculated according to Courtney (2000) as follows:

$$\sigma_{UTS,C} = \sigma_{UTS,RE} \times V_{RE} + \sigma_M\left(\epsilon^F_{RE}\right) \times V_M \quad (2)$$

$\sigma_M\left(\epsilon^F_{RE}\right)$ stands for the stress occurring within the matrix at fracture of the reinforcing element. The fracture of the reinforcing element marks the transition to region IV which represents the elastic-plastic behaviour of the remaining matrix until its final fracture. The ultimate tensile strength of the remaining matrix can be calculated from the volume weighted ultimate tensile strength of the matrix material according to Eq. (3):

$$\sigma_{IV} = V_M \times \sigma_{UTS,M} \quad (3)$$

It should be noted that these relationships are focussed on the use of ductile reinforcing elements resulting in higher tensile strengths than predicted by the models. This is due to the fact that the reinforced matrix impedes necking, or delays necking to higher stress, as discussed by Courtney (2000). The triaxial stress state must also be considered.

It has been found that multiple necking of the wire in the composite occurs during tensile loading of 11.1 vol.-% reinforced specimen. Hammers et al. (2010) investigated the influence of heat treatments and process routines on different composite systems with aluminium matrices for reinforced aircraft stringers, which showed different deformation and damage behaviour depending on the used matrix alloy and reinforcing element material. The state of the interfacial area was determined to be crucial for the reachable tensile strength and the resulting damage behaviour. Dependent on the damage behaviour the tensile strength was directly correlated to the debonding shear strength. Therefore in this work push-out

**Table 1**
Spectral Analysis of chemical composition of the materials used in wt-%.

| Elements | Si | Fe | Cu | Mn | Mg | Cr | Zn | Ti | Ni | Al |
|---|---|---|---|---|---|---|---|---|---|---|
| EN AW-6082 | 0.911 | 0.205 | 0.011 | 0.481 | 0.68 | 0.007 | 0.006 | 0.012 | 0.006 | Bal. |

| Elements | C | Si | Mn | P | S | Cr | Ni | Mo | N | Fe |
|---|---|---|---|---|---|---|---|---|---|---|
| 301SS | 0.074 | 0.52 | 0.93 | 0.034 | 0.002 | 18.2 | 8.3 | 0.43 | 0.043 | Bal. |

**Table 2**
Mechanical Properties of the EN AW-6082 matrix material.

| Heat treatment state | | E-Modul | $R_{p0.2}$ in MPa | $\sigma_{UTS}$ in MPa | $\epsilon^F_M$ in% |
|---|---|---|---|---|---|
| T4 | T4(F)$_a$ | 62 ± 3 | 114 ± 6 | 236 ± 4 | 25 ± 1 |
| | T4(F) | 65 ± 1 | 142 ± 4 | 280 ± 2 | 29 ± 5 |
| T6 | T6 | 66 ± 1 | 285 ± 2 | 311 ± 4 | 20 ± 3 |

**Table 3**
Mechanical Properties of the spring steel wires used (1.4310).

| | E-Modul | $R_{p0.2}$ in MPa | $\sigma_{UTS}$ in MPa | $\epsilon^F_{RE}$ in% |
|---|---|---|---|---|
| **As supplied** | 195.4 ± 4 | 1954 ± 42 | 2049 ± 90 | 2.1 ± 0.2 |
| **Heat treated**[a] | 194.8 ± 6 | 1952 ± 52 | 2130 ± 12 | 2.1 ± 0.1 |

[a] 530 °C for 1 h and 185 °C for 5 h.

tests were performed additionally to evaluate the influence of the heat treatment states on the debonding shear strength.

## 2. Materials and experimental details

### 2.1. Materials

The material used for the matrix (M) is the hardenable aluminium alloy EN AW-6082 (AlMgSi1). The reinforcing element (RE) is a spring steel wire (301SS). The measured chemical composition of the materials used is given in Table 1. The quasi-static properties of the matrix material are shown in Table 2. The quasi-static properties of the reinforcing element can be taken from Table 3. No changes of mechanical properties due to the heat influence during composite extrusion and additional heat treatment could be observed.

For the current investigations profiles with a cross-section of 40 × 10 mm$^2$ were produced via composite extrusion with a pressing ratio of 42:1. The block temperature was set to 550 °C and the profiles were pressed with a ram speed of 0.5 mm/s and an initial tool temperature of about 420 °C. As the block temperature is in the range of solution annealing temperature of the matrix material, the heat treatment could be done directly during fabrication. Therefore the quenching was done by an integrated system for quenching with moving air (index a) respectively by a setup for direct water quenching after extrusion, shown in Fig. 2. This setup allowed for quenching with a distance of only 300 mm in front of the outlet port of the extrusion press.

The investigated heat treatment states are shown in Table 4.

The composite profile was reinforced with 5 symmetrically arranged wires with a diameter of 1 mm resulting in a volume fraction of the profile of 0.98 vol.%. The unreinforced profiles where produced on the same run by cutting the reinforcing wires after producing the composite profiles. Fig. 3a) shows the cross-sections of the fabricated profiles in heat treatment state T4(F). The interface between wire and matrix appears to be free of macroscopic defects and shows a good optical bonding (Fig. 3b).

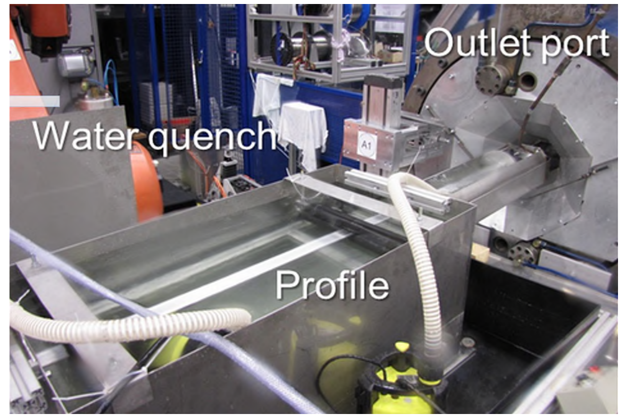


**Fig. 2.** Quenching setup for direct water quenching in front of the extrusion press (IUL Dortmund).

The specimen show a fine grain formation with an even finer microstructure around the steel wire and along the longitudinal welding seam (LWS) due to the higher local degree of deformation during the composite extrusion process (Fig. 3c). These illustrated conditions could be observed for all investigated heat treatment states and no significant change in grain size distribution was observed using light microscopy.

### 2.2. Specimen geometry and experimental setup

The specimens used for the tensile tests (Fig. 4) were cut out from the extrusion profiles. For the reinforced specimen the spring steel wire with a diameter of 1 mm is situated in the centre of the measuring gauge with a diameter of 3 mm resulting in a reinforcing fraction of 11.1 vol.% within the gauge length. For the tensile tests three specimens of each configuration were tested.

The tensile tests were carried out on a universal testing machine Zwick with a maximum load of 200 kN. The crosshead velocity was set to 1 mm/min resulting in a strain rate in the measuring gauge of 8.3 × 10$^{-4}$ l/s. The strain was measured using an extensometer.

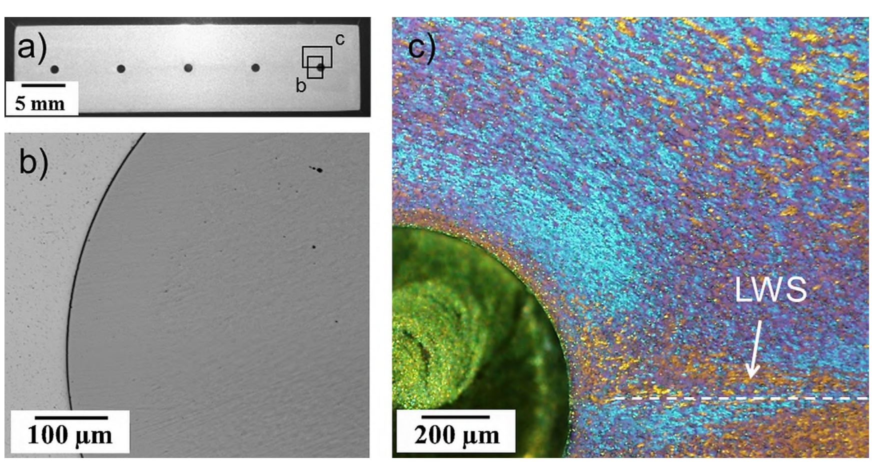


**Fig. 3.** a) Cross section of a 40x10 mm$^2$ profile reinforced with 5 spring steel wires (reinforcing ratio = 0.98 vol.-% after the composite extrusion process, heat treatment state T4(F) b) selected interface region c) grain size visualization with etching according to Barker (1950).

**Table 4**
Labelling of the different heat treatment states.

| Heat treatment-state | Solutionizing | Quenching | Ageing |
|---|---|---|---|
| $T4(F)_a$ | Solution annealing before composite extrusion | Quenching with air directly after the composite extrusion process | Natural ageing for more than 7 d |
| T4(F) | Solution annealing before composite extrusion | Quenching with water directly after the composite extrusion process | Natural ageing for more than 7 d |
| T6 | Solution annealing before composite extrusion | Quenching with water directly after the composite extrusion process | Artificial ageing for 5 h at 180 °C, 30 min after extrusion process |

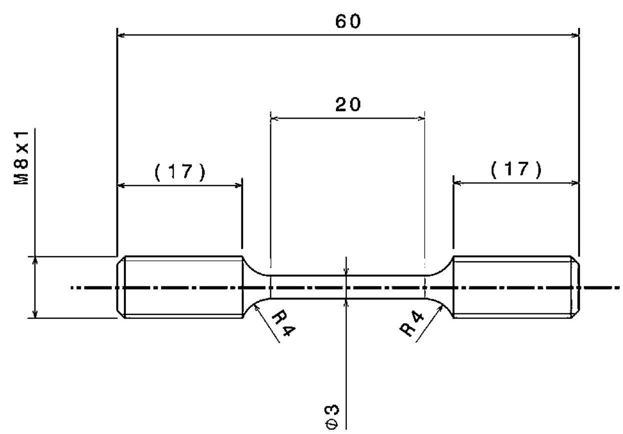


**Fig. 4.** Specimen geometry with position of the wire if reinforced (dashed line).

The hardness tests were performed in order to compare the heat treatment states with the requirements in DIN EN 755-2 (2008) and were carried out on a Brinell hardness testing machine with a test load of 62.5 kg and an indentation time of 10 s. Three indentations were measured per state in the cross-section orthogonal to pressing direction.

In order to determine the debonding shear stress along the interface between matrix and wire the push-out test, according to the technique described by Marshall (1984) and which was already applied on composite extruded materials by Weidenmann et al. (2006b) were performed on rectangular plates with a specimen thickness of 1 mm. The testing was carried out on a Zwick universal testing machine with a maximum load of 2.5 kN. 10 specimens were tested for each material state investigated.

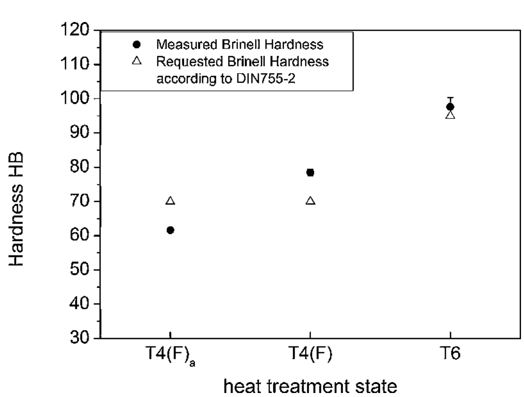


**Fig. 5.** Relation between Brinell hardness and heat treatment state and comparison to the requirements according to DIN EN 755-2 (2008).

## 3. Results

### 3.1. Brinell hardness measurements

In order to check the applied heat treatment steps Fig. 5 shows the measured Brinell hardness of the matrix material in different heat treatment states and the dedicated values requested by DIN EN 755-2 (2008). An adequate hardness could be reached only in the states T4(F) and T6 which were quenched with water during fabrication.

### 3.2. Tensile tests

Fig. 6a) shows the determined tensile properties for the unreinforced matrix material, i.e. the ultimate tensile strength $\sigma_{UTS}$ and the offset yield strength $R_{p0.2}$ compared to the requested values for T4 heat treatment state: $\sigma_{UTS}$ = 205 MPa and $R_{p0.2}$ = 110 MPa, for

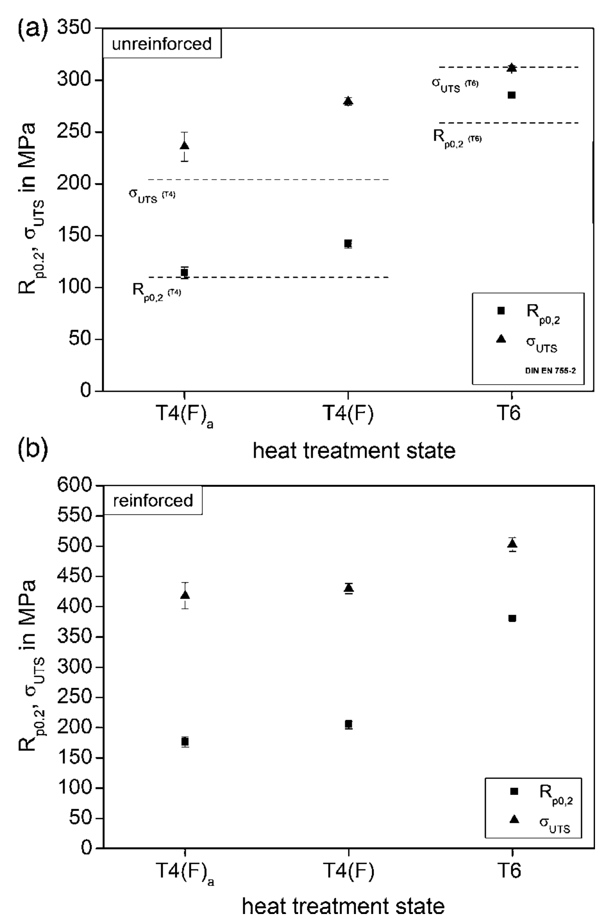


**Fig. 6.** Relation between $R_{p0.2}$, $\sigma_{UTS}$ and heat treatment state for matrix (a) and reinforced material (b).

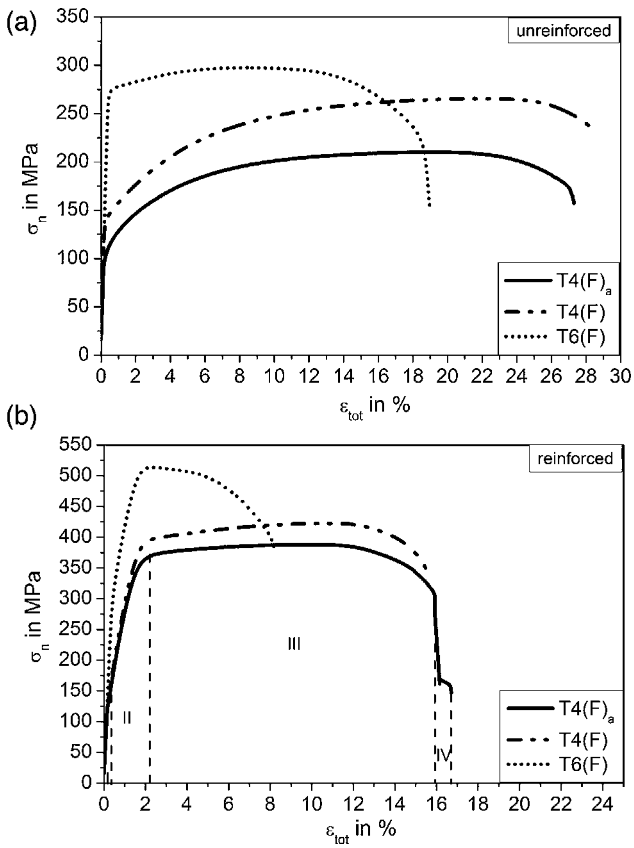


**Fig. 7.** Nominal stress-strain-curves of unreinforced (a) and the reinforced (b) specimen in different heat treatment states.

T6: $\sigma_{UTS}$ = 310MPa and $R_{p0.2}$ = 260 MPa from DIN EN 755-2 (2008) (dashed-lines). The requested values for T4 have been reached by both water and air quenching, whereas water quenched profiles show significantly higher values of $\sigma_{UTS}$ and $R_{p0.2}$. The increase in $\sigma_{UTS}$ by water quenching was determined to be 44 MPa (+18%) and in $R_{p0.2}$ to 38 MPa (+33%). Artificial ageing of the water quenched profiles leads to a gain of 32 MPa (+11%) in $\sigma_{UTS}$ and 144 MPa (+101%) in $R_{p0.2}$. Obviously the requested values are exceeded with relatively low fluctuations if the profiles were water quenched directly after extrusion, more fluctuations are observed by quenching with air.

Comparing the unreinforced matrix to the composite material shown in Fig. 6b), it turns out that the ultimate tensile strength ($\sigma_{UTS}$) and the offset yield strength $R_{p0.2}$ is significantly increased by the reinforcement. The influence of the heat treatment shows a reduction of fluctuations by using water as quenching medium accompanied by an increase in ultimate tensile strength $\sigma_{UTS}$ of 12 MPa (+3%) and offset yield strength $R_{p0.2}$ of 29 MPa (+17%). Artificial ageing (T6 state) leads to a further increase in ultimate tensile strength $\sigma_{UTS}$ of 73 MPa (+17%) and in the offset yield strength $R_{p0.2}$ of 175 MPa (85%) compared to reinforced T4(F)-state.

In order to get a detailed insight in the deformation and damage behaviour regarding the influence of the heat treatment state Fig. 7 shows stress-strain curves of the matrix and the composite.

Fig. 7a) shows the stress-strain curves for the unreinforced aluminium alloy where an increase in strength and ductility is observed for the T4(F) state compared to the T4(F)$_a$ state. The T6 state shows a significant increase in strength accompanied by a decrease of ductility. In comparison to both T4 states, the T6 state shows less plasic deformation potential, expressed by the smaller $\sigma_{UTS}$ to $R_{p0.2}$ ratio.

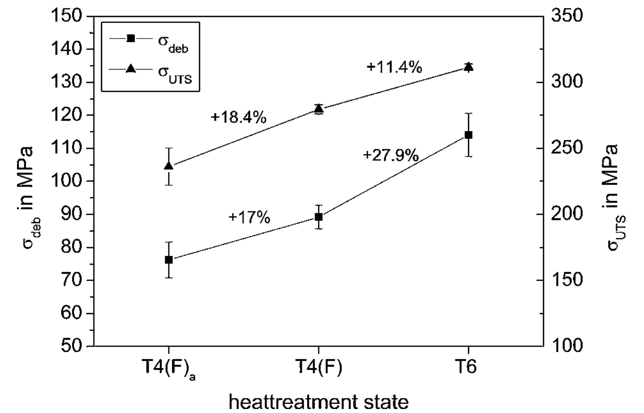


**Fig. 8.** Evolution of the debonding strength $\sigma_{deb}$ and ultimate tensile strength $\sigma_{UTS}$ measured for different heat treatment states.

The composite specimens tested (Fig. 7b)) show same tendencies regarding the strength values, while ductility (expressed by the total strain to wire fracture) is reduced compared to the unreinforced matrix. In agreement with the results from Kelly and Davies (1965), respectively Merzkirch et al. (2014), four regions of deformation can be distinguished and are illustrated for heat treatment state T(F)$_a$ in Fig. 7b).

It is worth mentioning that the T4 states show a distinctive plateau in region III where strain to fracture of the single wire, which is 2.1%, is significantly exceeded. Both T4 states show a comparable length of the plateau region. The T6 state shows a clear reduction of total strain to wire fracture compared to the T4 states, but nevertheless the total strain to fracture of the wire is also exceeded. Instead of a plateau region a continuous decrease of stress is observed after reaching the maximum stress.

### 3.3. *Push-out tests*

In order to evaluate the influence of heat treatment on the interfacial properties, push-out tests were performed for each heat treatment state. The measured debonding shear strengths can be seen in Fig. 8 (left axis).

The evolution of the debonding shear strength shows a considerable dependency on the heat treatment state. Water quenching leads to an increase of the debonding shear strength from 76 MPa to 89 MPa (+17%) and furthermore to an increase in debonding shear strength by artificial ageing by 27.9% to about 114 MPa.

As the failure mostly takes place in the matrix material the measured debonding shear strength $\sigma_{deb}$ was correlated with the measured ultimate tensile strength $\sigma_{UTS}$ of the matrix material (see Fig. 8 right axis).

Assuming a good bonding in the interfacial zone and shear failure in the matrix material the debonding shear strength should be dependent on the shear strength of the matrix and therefore should show an analogous correlation like between ultimate tensile strength and heat treatment state. By correlating the $\sigma_{deb}$ with $\sigma_{UTS}$ of the matrix material the influence of the heat treatment shows a good agreement comparing T4(F)$_a$ to T4(F). The increase of the debonding shear strength from T4(F) to T6 is significantly higher than expected by the measured increase in $\sigma_{UTS}$ of the matrix material.

### 3.4. *Metallographic investigations*

#### 3.4.1. *Tensile tests*

In order to describe the deformation and damage behaviour for (plateau) region III (see Fig. 7), longitudinal sections of tested spec-

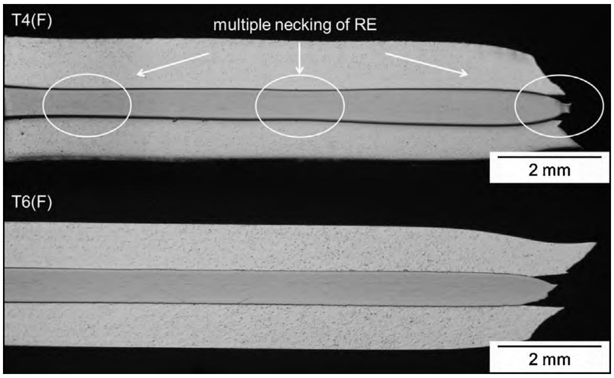


**Fig. 9.** Longitudinal optical micrographs of states T4(F) a) and T6(F) b) after fracture.

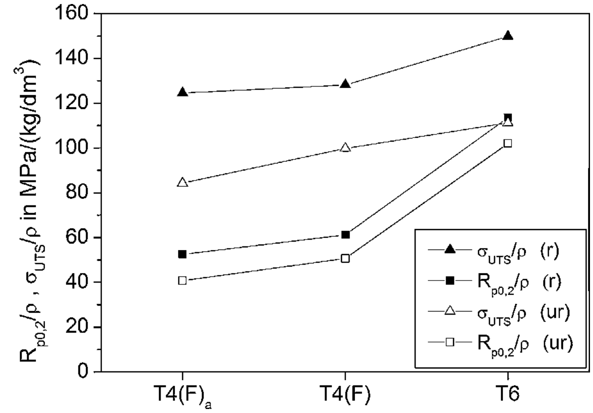


**Fig. 11.** Specific properties according to the heat treatment state.

imen have been investigated. Fig. 9 shows the longitudinal section of tested specimen in the heat treatment states T4(F) and T6. T4(F) specimens show three areas where advanced strain localisation (necking) of the reinforcing element and the matrix material occurs, which also was observed in $T4(F)_a$ specimens. These strain localisations lead to necking of the matrix material, which can be observed at the outer edge of the specimen. At the necked area where wire fracture occurred a delamination between wire and matrix can be observed.

In contrast T6 specimen does not show multiple necking and only one area of strain localisation which eventually caused the fracture of the composite. The remaining reinforcing element and the interface seem to be completely free of deformation and damage.

*3.4.2. Push-out tests*

In order to confirm the assumed failure mode during the push-out tests, selected longitudinal micrographs of tested push-out specimens were made. Fig. 9 shows a push-out specimen in heat treatment state T4(F).

Large areas of matrix material residues on the wire, as shown in Fig. 10 b) can be confirmed for all heat treatment states, whilst the percentage of aluminium residues in the T6 state was more or less equal. No indications for constitution of coarse intermetallic phases where found in any heat treatment state, but according to TEM-investigations by Weidenmann et al. (2006b) it is to be assumed that the chemical bond is characterized by a small diffusion zone off less than 1 μm.

## 4. Discussion

### *4.1. Mechanical properties*

In order to increase the specific and absolute strength and offset yield stress of reinforced composites the presented results showed that an adequate heat treatment, which has been introduced to the composite extrusion process, is an appropriate method for composite extruded aluminum profiles. Especially strong benefits through water quenching directly during the processing of composite profiles were shown. The presented investigations show that the choice of the heat treatment state has a high influence on the mechanical properties of the aluminum alloy EN AW-6082, and therefore affect the behaviour of the composite material in basically the same manner. Offset yield strength and ultimate tensile strength could considerably be increased by quenching with water in both cases: unreinforced and reinforced, which confirms the quench sensitivity of the aluminium alloy EN AW-6082. Furthermore residual stresses due to cooling have to be taken into account. Based on the thermal mismatch of matrix material and wire, positive residual stresses in the matrix and negative residual stresses in the wire are expected. This could explain the early onset of region II and therefore the measured increase in $R_{p0.2}$ (due to water quenching) of the reinforced material is slightly lower than of the matrix material (unreinforced: +33%/reinforced: +17%).

Fig. 11 gives an overview of the specific properties according to the heat treatment state. Whereas water quenching leads to an equal increase of the specific strength values $R_{p0.2\%}$ and $\sigma_{UTS}$, in heat treatment state T6 a vast improvement of the specific offset yield strength is observed.

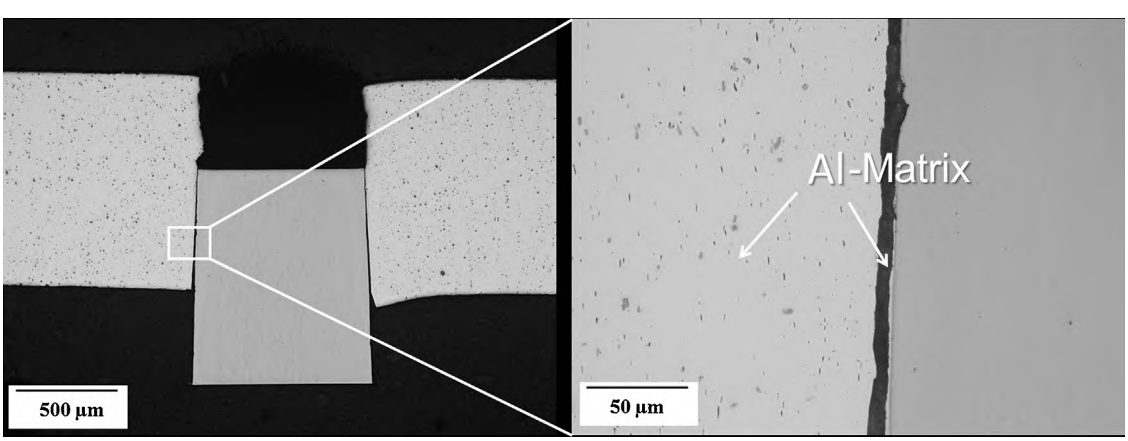


**Fig. 10.** Optical micrograph of a push-out specimen in state T4(F) and detailed view on the sheared interface region.

This gain applies to the unreinforced matrix-material (ur) as well to the reinforced composite material (r). As it can be seen the specific properties of heat treatment T6 (ur) are higher than the ones of heat treatment T4 (r), which may be sufficient for some applications and should be considered first. But nevertheless comparing heat treatment T6 (ur) and T6 (r) the benefit of the reinforcing wires is very obvious. It can be seen that the offset yield strength of the composite system exceeds the ultimate tensile strength of the unreinforced matrix material. Furthermore the hardening buffer between $R_{p0.2}$ and $\sigma_{UTS}$ is largely increased by the reinforcement in heat treatment state T6.

### *4.2. Interfacial mechanical properties*

The heat treatment state also affects the interfacial strength. As shown in optical micrographs the failure of the interface mainly takes place in the aluminum matrix. Therefore higher strength of the matrix material should improve the debonding shear strength which has been proved by push-out tests. Correlating the debonding shear strength with the ultimate tensile strength of the matrix material it can be noted that the increase of the deboning shear strength by water quenching corresponds with the increase in matrix strength. Whereas the relative increase by artificially ageing in debonding shear strength is significantly higher than assumed by the measured increase in the ultimate tensile strength of the matrix material. The reasons was not clarified yet, but is assumed to be an effect of improved diffusion bonding between wire and matrix, which will have to be further investigated. As a benefit of the fast processing time and no additional solution annealing time needed, no excessively forming of an intermetallic layer are found through light microscopic analysis like described by Pattnaik and Lawley (1974) or Hammers et al. (2010, 2013) but has to be investigated further using electron microscopic techniques.

### *4.3. Deformation and damage mechanisms*

A distinctive plateau region was observed in heat treatment states $T4(F)_a$ and T4(F), which showed an increase in strain to fracture of the reinforcing element and could be correlated to delamination and multiple necking of the reinforcing element by optical micrographs of tested specimen and was also observed in earlier investigations of Merzkirch et al. (2011, 2014). Additionally the necking of the matrix material in turn leads to a debonding of the interface between reinforcing element and matrix material (see Fig. 9).

In contrast, no multiple necking could be identified in the examined specimens of the T6(F) state. As described by Schoene and Scala (1970) and Venett et al. (1970) for tungsten reinforced brass composites and later by Weidenmann et al. (2006a), Merzkirch et al. (2014) and Hammers (2013) for aluminum steel wire composites, the necking of wire and subsequent necking of the matrix, leads to a simultaneous work hardening of the necked region in the matrix, which therefore enables the bypassing of the applied load around the debonded area. This allows for a multiple necking of the reinforcing element and leads in consequence to a much higher strain to failure as observed in the single reinforcing element. Final failure follows at the point where delamination between wire and matrix occours and no further stabilization of the necked wire is present.

This mechanism is in good agreement with the observed stress-strain diagrams and the results of the metallographic investigations for heat treatment states $T4(F)_a$ and T4(F). The stress-strain curves for the T6(F) state rather show no distinctive plateau section but a steady decrease in the nominal stress. However the strain to fracture of the single wire is clearly exceeded. In the T6 state the possibility for matrix strain hardening is reduced (yield ratio $R_{p0.2}/\sigma_{UTS}$ (T6(F)) = 0.75 → yield ratio $R_{p0.2}/\sigma_{UTS}$ (T4(F)) = 0.48) and a high debonding shear strength is observed. In combination of this the resulting reduction of the plateau section can be explained. First the high debonding shear strength leads to a stabilization of the wire. Necking therefore is initially delayed respectively reduced. The surrounding matrix only has a small buffer for hardening, so the briding effect observed in the T4 state can not be activated and the necking of this area accompanied by delamination between wire and matrix leads to final fracture of the composite.

## 5. Conclusions

- A significant increase in $R_{p0.2}$ and $\sigma_{UTS}$ by reinforcing the aluminium matrix with steel wires was attested.
- Further improvement in specific mechanical properties can be reached by implementing an adequate heat treatment, therefore water quenching is obligatory to reach best material properties.
- Interface failure takes mainly place in the matrix material, therefore improvement of mechanical properties of the matrix material leads to higher debonding shear strength as well.
- Strain to fracture of the reinforcing element is increased above its actual limits in all heat treatment states and is linked with the occuring deformation mechanisms:
  - The deformation mechanisms of the T4 heat treatment state is characterized by a pleatau region where the composite shows a large increase in strain with almost none strain hardening. This could be lead back to a briding of initially necked areas due to work hardening which results in multiple necking of the reinforcing element.
  - In heat treatment state T6 the no multiple necking is observed. Due to a small work hardening buffer of the matrix material no briding of the initially necked area can be activated. Nevertheless the high interface strength leads to a stabilization of the wire and therefore the wire fracture in the composite is well beyond its actual strain limit.

## Acknowledgement

This paper is based on investigations of the subproject A3 – "Material systems for reinforced and functional extruded profiles" – of the Transregional Collaborative Research Center/Transregio 10, which is kindly supported by the German Research Foundation (DFG). The authors would like to thank S. Tünte for contributing to the experiments.

## References

Barker, L.J., 1950. Revealing the grain structure of common aluminum alloy metallographic specimens. Trans. Amer. Soc. Metals 42, 347–356.
Courtney, T.H., 2000. Mechanical Behavior of Materials, 2nd edition. McGraw-Hill, Boston, pp. 244–293.
Dahnke C., Pietzka D., Haase M., Tekkaya A.E., 2014. Extending the Flexibility in the Composite Extrusion Process. International Conference on Manufacture of Lightweight Components (ManuLight2014).
DIN EN 755-2, 2008. Aluminium and aluminium alloys –Extruded rod/bar, tube and profiles –Part 2: Mechanical properties.
Edwards, G.A., Stiller, K., Dunlop, G.L., Couper, M.J., 1998. The precipitation sequence in Al–Mg–Si Alloys. Acta mater. 46 (11), 3893–3904.
Hammers T., 2013. Wärmebehandlung und Recken von verbundstranggepressten Luftfahrtprofilen. Doctoral thesis, Karlsruhe Institute of Technology (KIT), Karlsruhe, ISBN: 978-3-86644-947-3.
Hammers, T., Kerscher, E., Weidenmann, K.A., 2010. Mechanical properties of compound extruded aircraft stringer profiles under cyclic loading. Adv. Eng. Mat. 7, 584–586.
Kelly, A., Davies, J., 1965. The Principles of the fibre reinforcement of metal. Metall. Rev. 10, 37.
Kleiner, M., Schomäcker, M., Schikorra, M., Klaus, A., 2007. Herstellung verbundverstärkter Aluminiumprofile für ultraleichte Tragwerke durch Strangpressen. Mat.-wiss. u. Werkstofftechn. 35, 431–439.
Lim, C.Y., Shercliff, H.R., 1993. Quench sensitivity of aluminium alloy 6082. In: Technical Report. Cambridge University Department of Engineering Cambridge, UK, pp. 5–22.

Marshall, D.B., 1984. An Indentation method for measuring matrix-fiber frictional stresses in ceramic composites. Commun. Am. Ceram. Soc., 259–260.
Merzkirch M., 2012. Verformungs- und Schädigungsverhalten der verbundstranggepressten, federstahldrahtverstärkten Aluminiumlegierung EN AW-6082. Doctoral thesis, Karlsruhe Institute of Technology (KIT), Karlsruhe, ISBN: 9783866449336.
Merzkirch M., Reeb A., Weidenmann K.A., Schulze V., 2011. Charakterisierung des Verformungs- und Schädigungsverhaltens unidirektional drahtverstärkter Aluminium und Magnesiummatrixverbunde unter Zug und Druckbeanspruchung. Tagungsband zum 18. Symposium Verbundwerkstoffe und Werkstoffverbunde, Wielage, Bernhard (Hrsg.).
Merzkirch, M., Meissner, M., Schulze, V., Weidenmann, K.A., 2014. Tensile behavior of spring steel wire reinforced EN AW-6082. J. Compos. Mater.
Mrówka-Nowotnik, G., Sieniawski, J., 2005. Influence of heat treatment on the microstructure and mechanical properties of 6005 and 6082 aluminium alloys. J. Mat. Process. Tech. 162–163, 367–372.
Murayama, M., Hono, K., 1999. Pre-precipitate clusters and precipitation processes in Al–Mg–Si. Acta Mater. 47 (5), 1537–1548.
Pattnaik, A., Lawley, A., 1974. Effect of elevated temperature exposure on the structure stability, and mechanical behaviour of aluminium-stainless steel composites. Metall. Trans. 5, 111–122.
Pietzka D., 2013. Erweiterung des Verbundstrangpressens zu höheren Verstärkungsanteilen und funktionalen Verbunden.Dissertation, Technische Universität Dortmund.
Pietzka, D., Tekkaya, A.E., 2009. Verbundstrangpressen. Fortschr. Bericht. VDI. 2, 668.
Pietzka, D., Schikorra, M., Tekkaya, A.E., 2008. Embedding of alumina reinforcing elements in the composite extrusion process. Adv. Mater. Res. 43, 9–16.
Schoene, C., Scala, E., 1970. Multiple necking phenomena in metal composites. Metall. Trans. 1 (12), 3466–4369.
Venett, M., Stanley, M., Albert, P., 1970. Multiple necking of tungsten fibres in a brass-tungsten composite. Metall. Trans. B 1 (6), 1569–1575.
Voigt, W., 1887. Theoretische studien über die elastizitätsverhältnisse der krystalle. K1 34, 3–51.
Weidenmann, K.A., Kerscher, E., Schulze, V., 2006a. Mechanical properties of compound-extruded aluminium-matrix profiles under quasi-static loading conditions. Adv. Mater. Res. 10, 23–24.
Weidenmann, K.A., Kerscher, E., Schulze, V., Löhe, D., 2006b. Characterization of the interfacial properties of compound-extruded lightweight profiles using the push-out-technique. Mater. Sci. Eng. A 424, 205–211.